Bulletin of the Seismological Society of America, Vol 73, No 3, pp 723-734, June 1983

NUMERICAL EVALUATION OF NEAR-FIELD, HIGH-FREQUENCY RADIATION FROM QUASI-DYNAMIC CIRCULAR FAULTS

By Michel Campillo

ABSTRACT

We compute the near-field, high-frequency radiation from a circular crack expanding with constant rupture velocity and discuss the characteristics of the stopping phases. We then introduce rupture velocity jumps in the fracture process. The computed accelerations show the dominant role played by the rupture front kinematics. The high acceleration pulses are associated with sudden changes of the rupture velocity. For a sudden jump (or a sudden stop), there is no theoretical high-frequency limit to the spectral density of acceleration. In order to account for f_{max}, we introduce a smooth deceleration of the rupture front over a time t' in place of a sudden stop. This results in a spectral fall-off for frequencies greater than $1/t'$ and supports the interpretation of f_{max} as a source effect.

Introduction

There is no evident quantitative relationship between the complexity of strong motion records and the source characteristics. Recent attempts have been made using composite source models (Aki *et al.*, 1977; Boatwright, 1982) or models with complex kinematics (Boore and Joyner, 1978). We shall follow this last approach and use the general idea developed by Madariaga (1983) who relates the high-frequency radiation to the existence of jumps of velocity of the rupture front. We shall present some numerical evaluation of the seismic acceleration radiated by such kinematic discontinuities occurring during the growth of a circular crack. The calculation will use the discrete wavenumbers method. We restrict our study to the case of a strike-slip earthquake.

For practical reasons, this study will be done using a circular crack model. In fact, we shall see that its radiation is always equivalent to the one of a circular rupture front whose kinematics presents some discontinuities. The most obvious of these discontinuities are the beginning and the end of the rupture propagation in the case of a circular crack expanding with constant rupture velocity. The importance of these events on the seismic radiation has been shown in the far field (Madariaga, 1976) as well as in the near field (Archuleta and Hartzell, 1981).

In introducing velocity jumps, we make the assumptions that the rupture velocity changes simultaneously all along the rupture front, and that the entire rupture surface undergoes a jump in slip velocity. These assumptions have to be considered as conditions of self-similarity of the crack until it reaches its final radius. The self-similar crack model is useful because the behavior in the vicinity of the rupture front is well known. The expression of the slip is given by (Kostrov, 1964)

$$\Delta u(r, t) = \frac{\tau_e}{\mu} C\left(\frac{v}{\beta}\right) (v^2t^2 - r^2)^{1/2} \qquad r < vt \tag{1}$$

with

τ_e = the effective stress equal to the difference between initial prestress and frictional stress on the fault

β = the shear wave velocity
v = the rupture velocity
μ = the shear modulus
$C(v/\beta)$ = a numerical value depending on the ratio v/β and roughly equal to 1 for subsonic rupture.

This expression describes the expansion of a dynamic crack at constant velocity. The end of the rupture process is complicated by the healing. For the high-frequency radiation, the most interesting aspect of this behavior, as pointed out by Madariaga (1983), is the concentration of slip velocity just behind the rupture front. At time t, this concentration is given in the form

$$\Delta \dot{u}(r, t) \simeq \frac{\tau_e}{\mu} C\left(\frac{v}{\beta}\right)\left(\frac{vt}{2}\right)^{1/2} v(vt - r)^{-1/2} \qquad vt \gtreqqless r. \tag{2}$$

The source of high-frequency radiation is located in space and time at the singularities of the function $\Delta \dot{u}(r, t)$. If the waves emitted by each point of this source arrive continuously at an observer, there will not be any strong variation of the wave field seen by the observer. The important events in high-frequency radiation will be associated with second-order discontinuities of the slip velocity. An example of such a discontinuity is the first arrival of the wave emitted by the stopping of the rupture at the periphery of a circular crack (see Archuleta and Hartzell, 1981).

Method of Calculation

In order to characterize the near-field, high-frequency radiation in relation with the kinematics of the rupture front, we calculate the accelerations produced in a half-space. We use the method of Bouchon (1981) which consists in a discretization of the wave field in terms of horizontal wavenumbers. The fault is represented by an array of point sources, and the superposition of the elastic field radiated by all the elementary sources is done in the frequency-horizontal wavenumber domain. Each point source is associated with a slip function $\Delta u(r, t)$ which depends on the distance between the point considered and the point of initiation of the rupture. The same representation was used by Campillo and Bouchon (1983) to model the source of small seismic events. The interval between elementary sources is chosen to be smaller than one-sixth of the shortest wavelength considered. The calculation is made at equally spaced frequencies spanning the interval 0 to 5 Hz.

The Case of a Circular Crack with Constant Rupture Velocity

To compare our solution with the results of Archuleta and Hartzell, we have done a calculation for the same source-medium-receiver configuration. The method used by these authors is very different from ours. It consists of a time domain superposition of Green's functions convolved with the source time history. Each Green's function is computed using the technique described by Johnson (1974). The geometry of the problem is displayed in Figure 1. The medium wave velocities are: β = 3 km/sec for S waves and $\alpha = \sqrt{3 \times \beta}$ for P waves. The shear modulus is 3×10^{11} dyne/cm^2.

The displacement at each point of the source is given by

$$\begin{aligned}
&\Delta u(r, t) = 0 && t < t_0(r) \\
&\frac{\Delta u(r, t)}{u_0} = (v^2t^2 - r^2)^{1/2} && t_0(r) > t > t_1(r) \\
&\frac{\Delta u(r, t)}{u_0} = (v^2t_1(r)^2 - r^2)^{1/2} && t > t_1(r)
\end{aligned}$$

$$t_0(r) = \frac{r}{v}; \qquad t_1(r) = \frac{R}{v} + \frac{(R - r)}{\beta}; \quad u_0 = \frac{C(v/\beta)^{r}e}{(1 + v/\beta)\mu} \tag{3}$$

where R denotes the final radius of the crack.

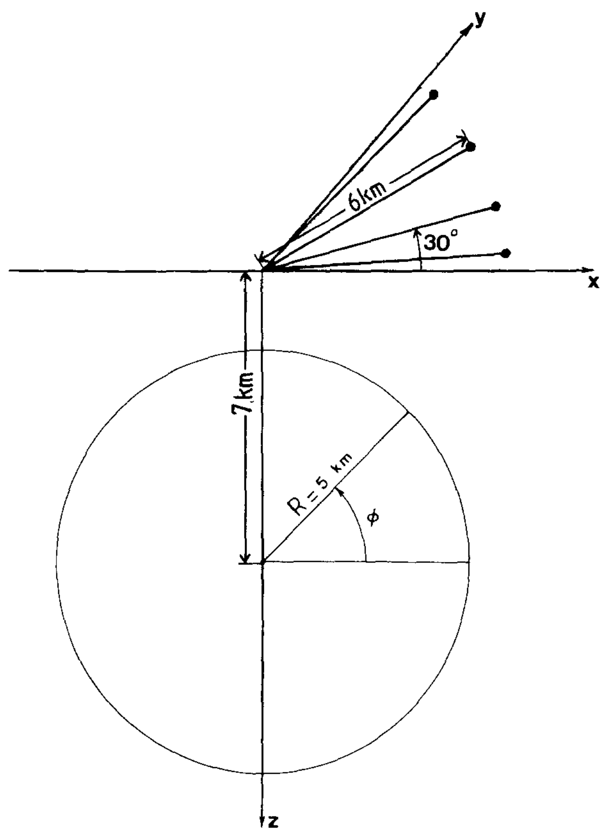

FIG. 1 Geometry of the source-receiver configuration.

This model represents a simple analytical approximation to the dynamic solution obtained by Madariaga (1976). Following Archuleta and Hartzell, we give the final slip at the hypocenter the value of 2.85 m. The rupture velocity is 0.75β, and the final source radius is 5 km.

The ground accelerations computed at an epicentral distance of 6 km and in an azimuth of 30° from the fault plane are presented in Figure 2 where they are compared to those obtained by Archuleta and Hartzell. U and V denote, respectively, the radial and tangential accelerations with respect to the epicenter. W is the vertical acceleration and is positive downward. There is a good agreement between the results obtained by the two methods both in the wave shapes and in the peak values. We note the noise level due to the sharp frequency cut-off used in the synthetics. We did not perform any signal processing to reduce this noise. This comparison shows a sufficient coherency to guarantee the accuracy of the two methods.

In order to assess the effect of the free surface, we also present in Figure 2 the infinite medium solution. The free surface amplifies the motion but does not produce any distortion of the wave shape. The three components of ground acceleration are characterized by two high-amplitude pulses. The first one (*fs*) corresponds to the arrival of the *S* wave emitted by the part of the rupture front the closest to the

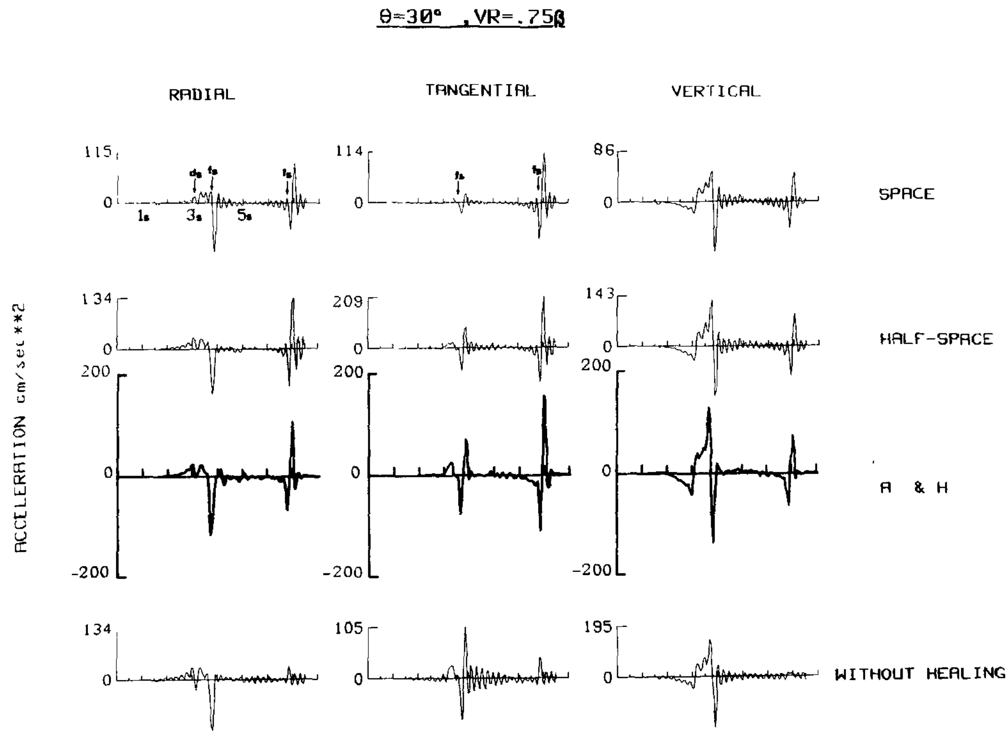

FIG. 2 Comparison between the computed accelerations obtained for the circular crack model using the discrete wavenumbers method in an infinite space and in a half-space with the results of Archuleta and Hartzell. The *lower trace* represents the solution for a circular source without healing, computed by the discrete wavenumber method.

observer at the time when the rupture propagation stops. The second pulse (*fs'*) is associated with the phase emitted at the same time but by the part of the rupture front the most distant from the observer.

The shapes of these two phases are, respectively, a delta-type impulse and a $1/t$ singularity. Their relative amplitudes are governed by the double-couple radiation pattern and the values of the directivity coefficient of the prominent polarized wave, and by the diffraction of the waves by the crack itself. This last point could be determinant when the head-wave associated with the crack surface (see Achenbach and Harris, 1978) appears.

The relative importance of the accelerations corresponding to arrivals emitted when the initiation occurs (*ds*) and when the expansion of the rupture stops depends on the azimuth of the observer and on the rupture velocity: (*ds*) appears to be stronger for higher rupture velocities. The phases associated with P-wave arrivals have low amplitudes and are difficult to identify on the synthetics.

Directivity of Ground Acceleration

Phase radiated from the nearest part of the fault. We have performed our calculations for three rupture velocities: 0.6β, 0.75β, and 0.9β in four azimuths: 5°, 30°, 60°, and 85° at the same epicentral range of 6 km. The amplitude of the stopping phase (fs) is strongly dependent on the rupture velocity, but the relationship between these two quantities is conditioned by the value of the angle Ψ between the directions of propagation of the rupture and wave fronts. We must thus take into account, in the interpretation of the synthetics, the effect of the possible coherency between rupture and wave fronts. The normalized amplitude of the phase (fs) measured on the tangential component is shown in Figure 3. Note that at an azimuth of 30°, the vertical component, which is prominent for this phase, displays the same increase with rupture velocity as the tangential component. The increase is stronger when Ψ is smaller.

In the case of a simultaneous velocity jump of a rupture front from v_1 to v_2, Madariaga (1977) gives the following approximate expression for the radiated acceleration pulse

$$u^i(R, \theta, \omega) = u_0{}^i(R, \theta, \omega, \Psi) \times (f(v1, \Psi) - f(v2, \Psi)) \tag{4}$$

where i denotes SH, SV, or P wave, f is the classical directivity factor (Ben-Menahem, 1961)

$$f(v, \Psi) = \frac{v}{\left(1 - \frac{v}{c_j} \cos \Psi\right)}$$

and c_j indicates S- or P-wave velocity.

In our study, it is not possible to speak in terms of polarized waves. The nearest part of the rupture front does not represent an in-plane or antiplane case (except for singular values of θ). For example, at 30° of azimuth from the fault plane (and for a strike-slip earthquake), the maximum acceleration occurs, for the phase (fs), on the vertical component in a half-space and on the radial component in an infinite space. There is, in this direction, a prevalence of the SV waves.

We have drawn in Figure 3 the normalized curve $f(v, \Psi)$ for SH wave. For the azimuth 5° and 85° with regard to the fault plane, which are the nearest ones to the nodal plane of the hypocentral double-couple, the f curves lie above our observations. This is explained by the fact that a rupture velocity increase induces a growth in the high-frequency content of the signal. Our high-frequency cut-off (5 Hz) is, therefore, the cause of this gap. At 60° of azimuth the behavior is exactly described by the f curve. The discrepancy observed at 30° from the fault plane may be caused by the absence of a constant polarization of the S wave. A stronger increase at high rupture velocity is typical for SV wave (in-plane shear crack for which the rupture velocity limit is the Rayleigh wave velocity). The general agreement between numerical solution and simple interpretation by the way of the directivity factor shows that the diffraction does not play an important part for this phase.

Phase radiated by the most distant part of the fault. The dependence of the directivity function f on azimuth and rupture velocity is considerably different when rupture and wave fronts are prograde, like in the case that we have just studied, or when they are retrograde. For phases coming from the most distant part of the fault, the fronts are typically retrograde. The directivity function then only takes values in the range of 0 to 1, whereas for prograde fronts its value lies between 1 to infinity. This behavior could be used to argue that the stopping phase from the farthest part of the fault should be weak. However, the diffraction factor can be very important in this case: such an example is shown in Figure 2. The stopping phase (fs') has here a large amplitude.

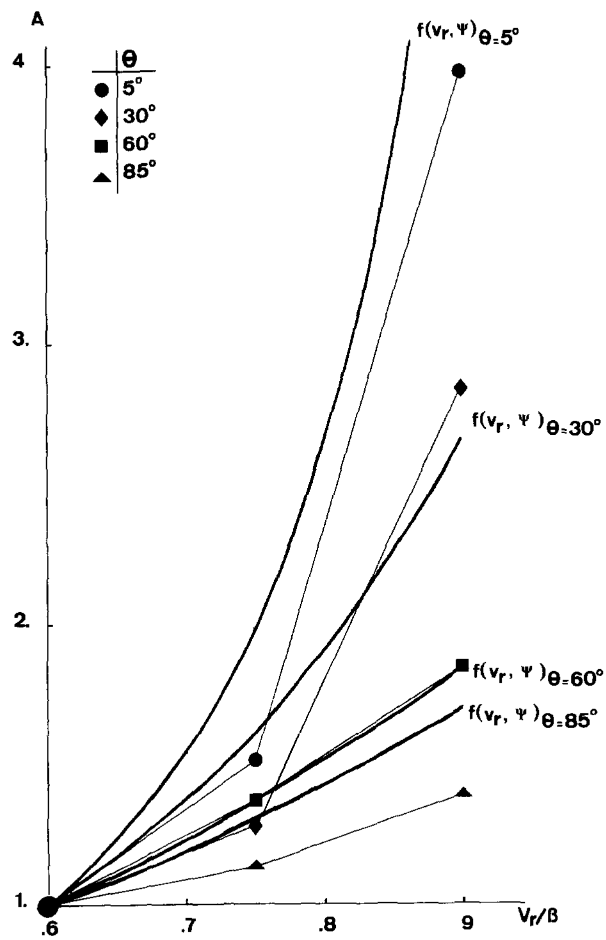

FIG. 3 Normalized amplitude of the fs phase acceleration pulse as a function of rupture velocity in different azimuths. The approximative directivity function f (see text) is shown for comparison.

This is explained by the particular azimuth of the receiver with respect to the rupture front propagation (124.2°), which is close to the direction of emission of the headwave associated with the crack surface. This direction is defined by $\Psi_{HW} = \cos^{-1}(-\beta/\alpha)$ (Achenbach and Harris, 1978), i.e., 125.7° in this case. The strength of this phenomenon is further enhanced by the presence in our model of a "healing phase," which propagates inward from the periphery of the crack and freezes the slip along its front. We can see in Figure 2 (*bottom trace*) that, in the absence of healing, the amplitude of this phase is much weaker. Its radiation pattern is, therefore, strongly dependent on the slip-time function.

A Circular Crack with Sudden Jumps of the Rupture Velocity

Until now, we have mainly studied the phase emitted from the final periphery of the fault when the expansion stops. This represents a jump of the rupture velocity from v to 0. We shall now consider the case where other rupture velocity jumps occur during the breakage. The presence of such jumps is a cause of incoherency, which leads to a high-frequency radiation. The enhancement of high frequencies by incoherent rupture processes has been discussed by Boore and Joyner (1978). Using the previous fault configuration, we have computed the ground acceleration associated with a sudden acceleration or deceleration of the crack tip.

In such a model of self-similar crack, the slip function takes the form

$$\Delta u(r,t) = 0 \qquad t < t_0(r)$$

$$\frac{\Delta u(r,t)}{u_0} = (v_1^2 t^2 - r^2)^{1/2} \qquad t_0(r) < t < t_c$$

$$\frac{\Delta u(r,t)}{u_0} = (v_2^2 (t - t_D)^2 - r^2)^{1/2} \qquad t_c < t < t_1(r)$$

$$\frac{\Delta u(r,t)}{u_0} = (v_2^2 (t_1(r) - t_D)^2 - r)^{1/2} \qquad t > t_1(r)$$

$$t_0(r) = \frac{r}{V_1} \quad t_0(r) < t_c$$

$$= t_c - \frac{(r - t_c V_1)}{V_2} \quad t_0(r) > t_c$$

$$t_c = \frac{R}{2V_M}; \qquad t_D = t_c\left(1 - \frac{V_1}{V_2}\right); \qquad t_1(r) = \frac{R}{V_M} + \frac{R - r}{\beta}$$

$$V_M = \frac{V1 + V2}{2}. \tag{5}$$

In all the cases studied, we assume the same final value of slip at the hypocenter. We have done the calculation for the same source-observer configuration as the one previously studied and have considered two cases

case SC1 with $V_1 = 0.6\beta$ and $V_2 = 0.9\beta$

case SC2 with $V_1 = 0.9\beta$ and $V_2 = 0.6\beta$.

The tangential accelerations obtained are depicted in Figure 4. In the case of a sudden acceleration (SC1), the initiation phase (ds) is very weak (compared with Figure 2). At 60° and 85° of azimuth, the disturbance corresponding to the wave emitted during the rupture velocity change, denoted by (c), is clearly seen; while for 5° and 30° (c) and (fs) are not distinguishable because their arrival times are very close. The (c) phase amplitude appears smaller than the (fs) one. Two factors account for this behavior. The first one is clearly expressed by equation (4): the jump of the directivity function is obviously larger when the velocity changes from 0.9β to 0 than when it changes from 0.6β to 0.9β. The second factor is that, in a dynamic crack model, the slip velocity near the rupture front is proportional to the stress intensity factor, which increases as the square root of the distance from the hypocenter. As in the case of a crack with a constant rupture velocity, the phase (fs') is very important at 30° of azimuth. The absence (or weakness) of a similar phase associated with the rupture velocity jump can be explained by the absence, in this case, of a healing phase. We have seen the importance of healing for the diffraction in the last section.

In the case of a sudden deceleration (SC2), the initiation phase (ds) is strong and has an amplitude comparable to the phase associated with the rupture velocity change (c). The acceleration which is produced by the stopping phase (fs) now has a much lower amplitude; it is associated with a smaller change of rupture velocity than in the case SC1. The importance which is now taken by the phase (c), with regard to the stopping phase (fs), is well explained by the properties of the directivity function. The change of value of this function is not simply related to the height of the jump: $|f(0.6\beta, \Psi) - f(0.9\beta, \Psi)|$ is greater than $|f(0.6\beta, \Psi) - 0.0|$ for any angle $|\Psi| < 56°$. The polarity of the pulse (c) is opposite for the two models.

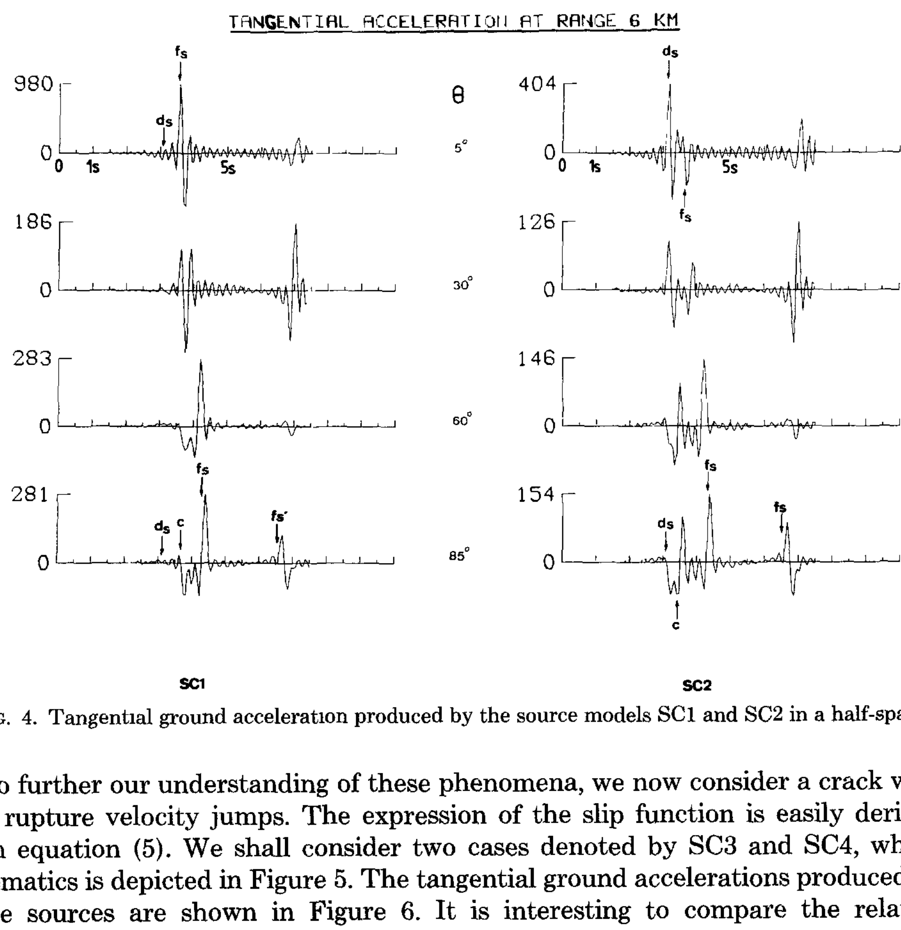

FIG. 4. Tangential ground acceleration produced by the source models SC1 and SC2 in a half-space

To further our understanding of these phenomena, we now consider a crack with two rupture velocity jumps. The expression of the slip function is easily derived from equation (5). We shall consider two cases denoted by SC3 and SC4, whose kinematics is depicted in Figure 5. The tangential ground accelerations produced by these sources are shown in Figure 6. It is interesting to compare the relative amplitudes of the different phases in these two cases: in the case SC3 and at an azimuth of 85°, (c_1), (c_2), and (fs) have similar amplitudes while at 5° (c_2) is the prominent pulse. On the contrary, in the case SC4, the stopping phases strongly prevail. These calculations show that the events which produce the high acceleration pulses are the rupture velocity jumps from or to a high rupture velocity, especially for observers near the fault plane, as we can foresee from Figure 3. The azimuthal dependence of signal shape and amplitude is very strong. At locations close to the fault strike, the accelerations are characterized by higher amplitude but less numerous pulses than at sites more distant from the fault plane. Consequently, the complexity of the rupture process is better represented by off-strike recordings where the phases associated with various rupture events are more equally weighted. On-strike, the acceleration signal is completely dominated by the phases associated

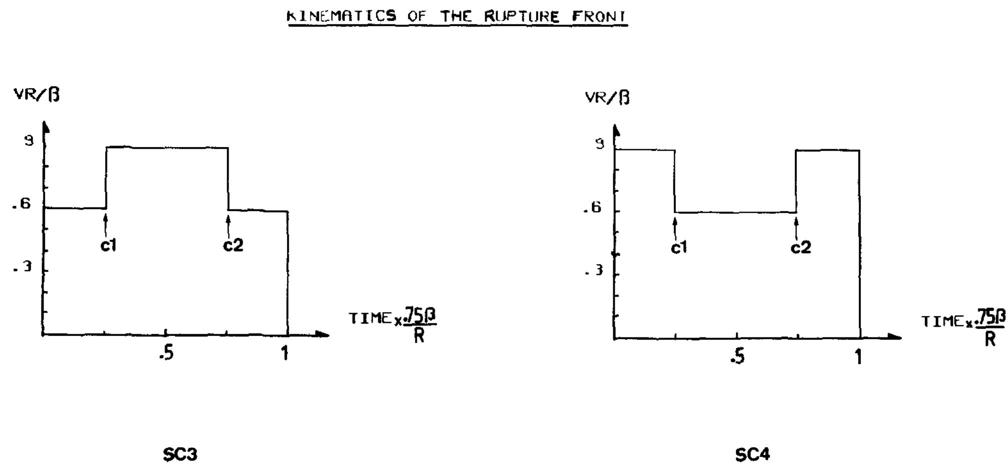

FIG 5. Kinematics of the rupture front for the source models SC3 and SC4.

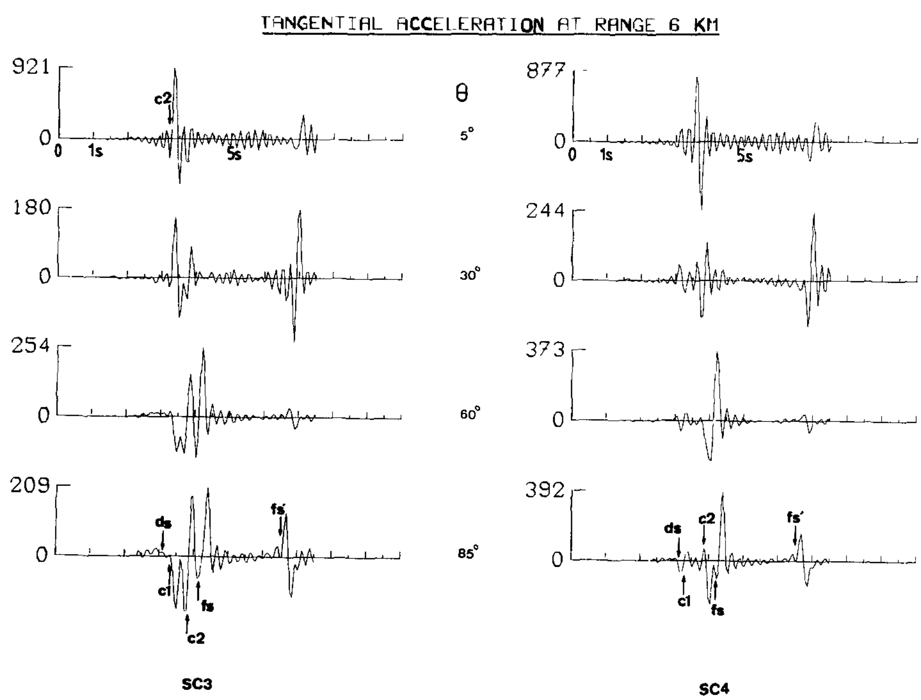

FIG 6. Tangential ground acceleration produced by the source models SC3 and SC4.

with the highest rupture velocities. The radial and vertical components of acceleration, not shown on the figure, display similar characteristics.

In order to illustrate this behavior, we compare in Figure 7 on-strike and off-strike recordings of the 1979 Imperial Valley earthquake. The accelerograms considered are those obtained at the El Centro Array No. 6 (component 230°) and Holtville (component 225°) stations. The maximum accelerations are recorded on-strike. These signals are made up of several pulses whose number and peak values may be regarded as characteristic of the source complexity. The number of pulses with amplitude larger than half the peak value for each signal is greater in the case of the off-strike station (13) than in the case of the on-strike receiver (5). Although nonunique, a model with several rupture velocity changes would account for these features.

High-Frequency Behavior of the Seismic Acceleration Spectrum

Until now, we have assumed that the rupture velocity jumps (or the stop of the crack expansion) are instantaneous. We have seen that these sudden jumps are responsible for acceleration pulses radiated by the source. In order to explain the high-frequency behavior of the observed accelerograms, namely the existence of a

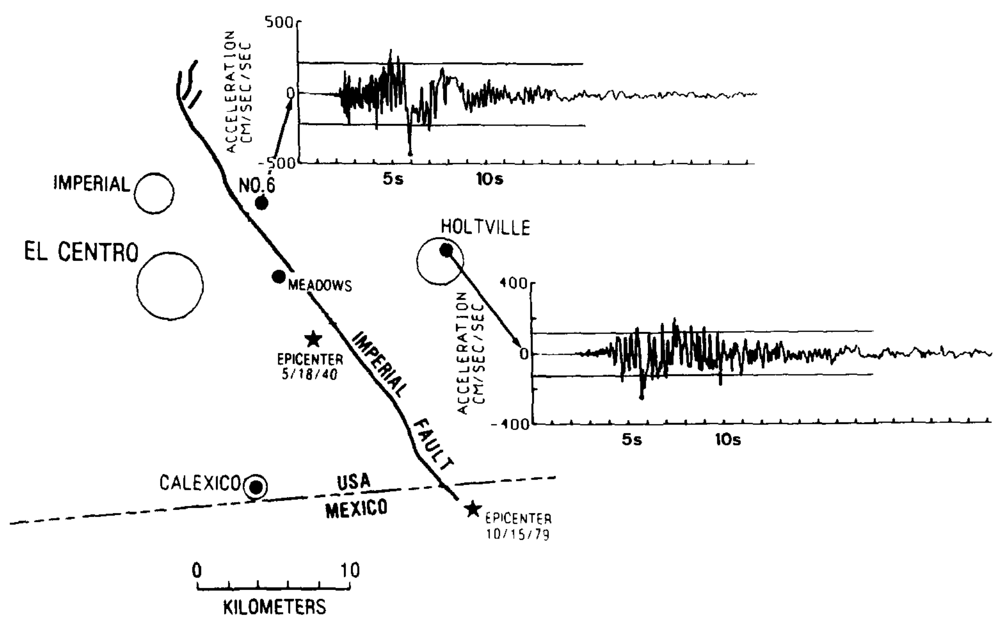

Fig 7 Strong motion stations in the Imperial Valley, California, and accelerograms from the 15 October 1979 earthquake (from Brady *et al*, 1980)

natural cut-off frequency f_{max} (Hanks, 1982), Boatwright (1982) has introduced, in his far-field representation, a finite width of the acceleration pulse, which he assumes to be directly related to the duration of the velocity jump. We present now some near-field calculations for crack models with smooth decelerations. Following Aki (1979), we associate such an evolution of the rupture velocity with a spatial change of the fracture energy of the medium.

We have considered two models with a rupture velocity of 0.75β different by the duration of the final deceleration: $t' = 1$ sec and $t' = 0.3$ sec. The computed acceleration spectra are depicted in Figure 8. They are compared with the case of a sudden stop. The high-frequency behavior is strongly affected: a large discrepancy of energy occurs beyond $1/t'$. This result suggests a relation between the duration t' or the corresponding distance covered by the decelerating crack tip $1'$ with the natural cut-off frequency currently denoted by f_{max}. Like the corner frequency which is related to the characteristic source dimension (or total rupture duration), f_{max}

seems related to another characteristic of the rupture process: the spatial extent of the rupture velocity jump (or its duration). The meaning of the corner frequency is clearly established for the circular crack model, for which Madariaga (1976) proposes a relation between this parameter, the radius of the crack, the rupture velocity, and the azimuth of the receiver. On the other hand, it is difficult to interpret physically the existence of f_{max}. An interpretation, which is suggested by this study, is that f_{max} is a measurement of the time of increase, up to a critical value, of the rate of energy absorbed by the tip of a growing crack. Such an interpretation is supported by the

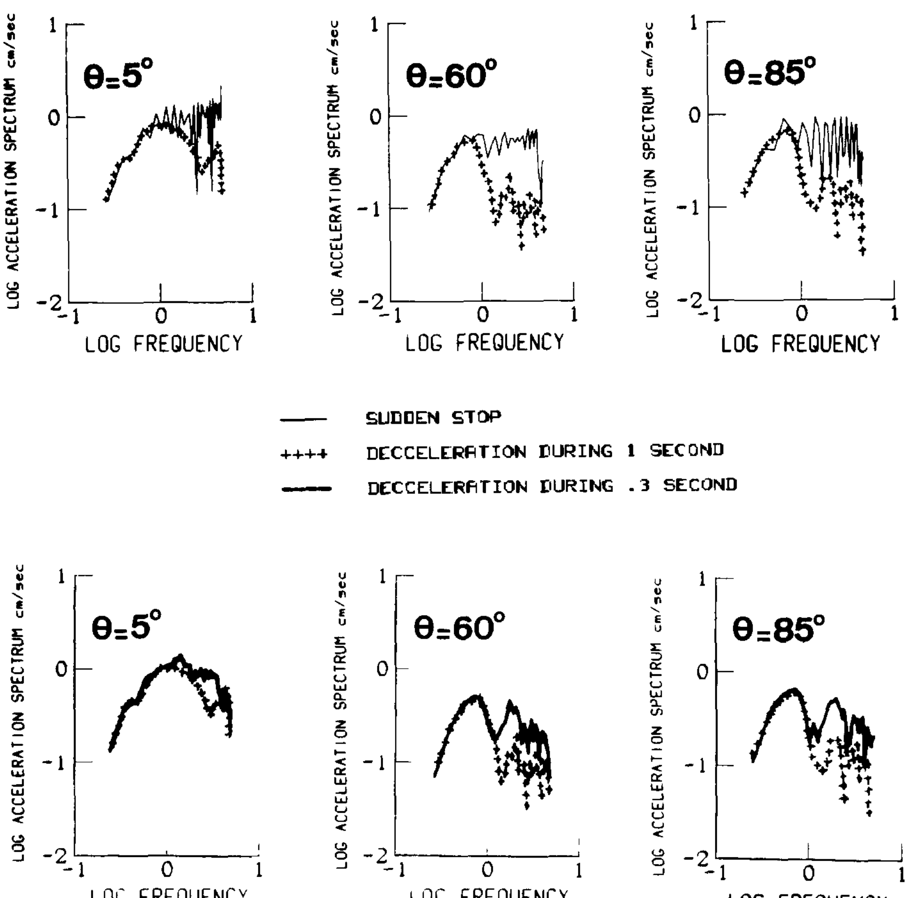

FIG 8. Acceleration spectra at a range of 6 km obtained for three different stopping processes The geometry of the crack is the one shown in Figure 1.

dynamic calculations performed by Nur and Israel (1979) which show the inverse relationship between local rupture velocity and rate of energy absorbed at the crack tip.

Concluding Remarks

In order to account for the observer complexity of the rupture processes, we have introduced in the classical crack model some jumps of the rupture velocity, and we have seen that these kinematic discontinuities are related to ground acceleration pulses. The ratio of peak acceleration to root mean square acceleration, R_A, seems to be an increasingly used characteristic of strong ground motions. By analogy with the work of Hanks and McGuire (1981), we have calculated this ratio for a time window starting from the arrival time of the first S wave and whose width is the rupture duration. We have done this calculation for the transverse component of the synthetics at 5° of azimuth with respect to the fault plane. In the case of a crack propagating with a constant rupture velocity (0.75β) and suddenly stopping, we have obtained $R_A = 3.7$. If we introduce a sudden jump of the rupture velocity, the value of R_A falls to 2.4. These values are coherent with the data compiled by Hanks and McGuire (1981) which show that R_A lies between 1.8 and 4.5 for California earthquakes. Another parameter which affects R_A is the high-frequency cut-off. Our synthetics show such a dependence: $R_A = 3.7$ for $f_{\max} = 5$ Hz, $R_A = 3.4$ for $f_{\max} = 3.3$ Hz and $R_A = 2.8$ for $f_{\max} = 1$ Hz. Nevertheless, the observed values of $f_{\max}$ (around 10 Hz) for great or moderate earthquakes show that low values of R_A cannot be explained by processes such as decelerations. Kinematic complexity seems to be the reliable characteristic of R_A.

Acknowledgments

I am indebted to Michel Bouchon for the help and attention that he provided throughout this work. I thank R. Madariaga and R. Archuleta for enlightening discussions. This work has been critically reviewed by J. Boatwright and D Boore. This research was supported by Institut National d'Astronomie et de Géophysique through Contract ATP-Sismogenèse

References

Achenbach, J D. and J. G. Harris (1978) Ray method for elastodynamic radiation from a slip zone of arbitrary shape, *J. Geophys. Res.* **83**, 2283–2291.

Aki, K (1979) Characterization of barriers on an earthquake fault, *J Geophys. Res.* **85**, 6140–6148.

Aki, K., M Bouchon, B. Chouet, and S. Das (1977) Quantitative prediction of strong motion for a potential earthquake fault, *Ann. Geophys.* **XXX**, 341–358.

Archuleta, R. and S. Hartzell (1981). Effects of fault finiteness on near source ground motion, *Bull. Seism. Soc. Am* **71**, 939–957.

Ben-Menahem, A (1961). Radiation of seismic surface waves from finite moving sources, *Bull. Seism. Soc. Am* **51**, 401–435.

Boatwright, J. (1982). A dynamic model for far-field accelerations, *Bull. Seism. Soc. Am.* **72**, 1049–1068.

Boore, D. M. and W. B. Joyner (1978). The influence of rupture incoherence on seismic directivity, *Bull. Seism. Soc. Am.* **68**, 283–300.

Bouchon, M. (1981). A simple method to calculate Green's functions for elastic-layered media, *Bull. Seism Soc Am* **71**, 959–971.

Brady, A. G., V Perez, and P. N. Mork (1980). The Imperial Valley earthquake, October 15, 1979, Digitalization and processing of accelerograph records, *U S. Geol. Surv., Open-File Rept. 80–703*, 1–309.

Campillo, M and M Bouchon (1983). A theoretical study of the radiation from small strike-slip earthquakes at close distances, *Bull Seism. Soc. Am.* **73**, 83–96.

Hanks, T. C. (1982). $f_{\max}$, *U.S. Geol. Surv , Open-File Rept. 82–591*, 405–436.

Hanks, T. C. and R. K. McGuire (1981). The character of high-frequency strong ground motion, *Bull. Seism. Soc. Am.* **71**, 2071–2095.

Johnson, L. R. (1974). Green's function from Lamb's problem, *Geophys J* **37**, 99–131.

Kostrov, B. V (1964) Self similar problems of propagation of shear cracks, *J. Appl. Math. Mech* **28**, 1077–1078.

Madariaga, R. (1976). Dynamics of an expanding circular fault, *Bull Seism. Soc. Am.* **66**, 639–666.

Madariaga, R. (1977). High frequency radiation from crack (stress drop) models of earthquake faulting, *Geophys. J. Roy. Astron. Soc.* **51**, 625–651.

Madariaga, R (1983). A string model for the high frequency radiation from earthquake faulting, *U.S. Geol Surv , Open-File Rept. 82-599*, 30–50.

Nur, A and M Israel (1980). The role of heterogeneities in faulting, *Phys. Earth Planet. Interiors* **21**, 225–236.

Laboratoire de Geophysique Interne
I.R I.G.M. BP 53 X 38041
Grenoble Cedex, France

Manuscript received 7 June 1982